

## THE HEAVY-ION COMPOSITIONAL SIGNATURE IN $^3\text{He}$ -RICH SOLAR PARTICLE EVENTS<sup>1</sup>

G. M. MASON

Department of Physics and Astronomy, University of Maryland

D. V. REAMES

NASA/Goddard Space Flight Center

B. KLECKER AND D. HOVESTADT

Max-Planck-Institut für Physik und Astrophysik

AND

T. T. VON ROSENVINGE

NASA/Goddard Space Flight Center

Received 1985 July 5; accepted 1985 October 10

### ABSTRACT

A survey of the  $\sim 1$  MeV per nucleon heavy-ion abundances in 66  $^3\text{He}$ -rich solar particle events has been performed using the Max-Planck-Institut/University of Maryland and Goddard Space Flight Center instruments on the *ISEE 3* spacecraft. The observations were carried out in interplanetary space over the period 1978 October–1982 June. We confirm earlier observations which show an enrichment of heavy ions in  $^3\text{He}$ -rich events, relative to the average solar energetic particle composition in large particle events. For our survey near 1.5 MeV per nucleon the enrichments compared to large solar particle events are approximately  $^4\text{He}:\text{C}:\text{O}:\text{Ne}:\text{Mg}:\text{Si}:\text{Fe} = 0.44:0.66:1.:3.4:3.5:4.1:9.6$ . Surprising new results emerging from the present broad survey are (1) the heavy-ion enrichment pattern is the same within a factor of  $\sim 2$  for almost all cases, and (2) the degree of heavy-ion enrichment is uncorrelated with the  $^3\text{He}$  enrichment. Overall, the features established here appear to be best explained by an acceleration mechanism in which the  $^3\text{He}$  enrichment process is *not* responsible for the heavy-ion enrichment, but rather the heavy-ion enrichment is a measure of the ambient coronal composition at the sites where the  $^3\text{He}$ -rich events occur.

*Subject headings:* cosmic rays: abundances — particle acceleration — Sun: abundances — Sun: corona — Sun: flares

### I. INTRODUCTION

Solar energetic particle events rich in  $^3\text{He}$  represent one of the most extreme fractionation processes known to occur in astrophysical sites, and as such may yield important clues to conditions in the solar corona and to the mechanisms of particle acceleration in solar flares. This class of particle events was first identified from their  $^3\text{He}/^4\text{He}$  ratios of a few percent to greater than one (Hsieh and Simpson 1970; Dietrich 1973; Garrard, Stone, and Vogt 1973; Anglin 1975; Serlemitsos and Balasubrahmanyam 1975; Hempe *et al.* 1979). These large  $^3\text{He}/^4\text{He}$  ratios represent an enrichment of  $10^3$ – $10^4$  over typical coronal and solar wind values (e.g., Geiss and Reeves 1972; Coplan *et al.* 1984) of  $5 \times 10^{-4}$ . Hurford *et al.* (1975) showed that there was a tendency for  $^3\text{He}$ -rich events to be enriched in elements with  $Z \geq 6$ , and subsequent work with more advanced instrumentation established that the enriched heavy nuclei covered the range through Fe (Hovestadt *et al.* 1975; Gloeckler *et al.* 1975; Anglin, Dietrich, and Simpson 1977; Zwickl *et al.* 1978; McGuire, von Rosenvinge, and McDonald 1979*b*; Mason, Gloeckler, and Hovestadt 1979*a, b*; Mason *et al.* 1980; Reames and von Rosenvinge 1981; Möbius *et al.* 1980, 1982), and that the element carbon was sometimes

strongly depleted (Mason, Gloeckler, and Hovestadt 1979*a, b*; Mason *et al.* 1980). Ramaty *et al.* (1980) and Kocharov and Kocharov (1984) have reviewed many features of these events.

The association of heavy-ion enrichments with the enrichment of  $^3\text{He}$  has important implications for particle acceleration mechanisms invoked to explain the  $^3\text{He}$ -rich events. Thus, models which produce enrichments of  $^3\text{He}$  through spallation or thermonuclear reactions (see discussion in Ramaty *et al.* 1980) were generally discarded in part because they contained no mechanisms for enriching heavy nuclei. In addition, the spallation models could not explain extreme cases with  $^3\text{He}/^4\text{He} \gtrsim 1$  simultaneously with only small upper limits for  $^2\text{H}$  and  $^3\text{H}$ . On the other hand, plasma heating mechanisms which selectively heat  $^3\text{He}$  can also selectively heat heavy ions under certain conditions. One set of such models has been proposed by Ibragimov and Kocharov (1977) and Kocharov and Orishchenko (1983, 1985), although Weatherall (1984) has questioned basic assumptions in these models which bear directly on their ability to selectively heat heavy ions. Another model using ion-cyclotron waves (Fisk 1978; Varvoglis and Papadopoulos 1983) can achieve selective preheating of  $^3\text{He}$  and also partially stripped heavy ions. Experimental measurements of the ionization states of heavy ions measured during a single  $^3\text{He}$ -rich event lend some support to the ion-cyclotron wave models (Ma Sung *et al.* 1981).

Previous studies of heavy-ion enrichments in  $^3\text{He}$ -rich events covered only a few isolated cases, making it difficult to discern systematic features associated with the heavy-nuclei

<sup>1</sup> This work was supported in part by the National Aeronautics and Space Administration under contract NAS5-28704 and grants NGR 21-002-224/316 and NAGW-101, by the National Science Foundation under grant ATM-84-07546, and by the Bundesministerium für Forschung und Technologie, FRG, contract RV 14-B8/74.

enrichments. In order to explore more thoroughly the properties of these enrichments we have undertaken a survey of the heavy-nuclei abundances in 66  $^3\text{He}$ -rich events which occurred during the period 1978 October–1982 June. The most surprising result of the study is the discovery that there exists a *characteristic* heavy-ion enrichment pattern in these events that is remarkably constant (generally within a factor of 2) from one event to the next, *independent* of the degree of  $^3\text{He}$  enrichment. The heavy-ion enrichments also appear to be independent of energy or spectral index, thus suggesting that the enrichments exist in the coronal material *before* acceleration to the  $\sim\text{MeV}$  energies observed in interplanetary space. Our observations of an association of heavy-ion enrichments with  $^3\text{He}$  enrichment are compatible with the plasma resonance models mentioned above. However, we suggest that the lack of detailed correlation between the  $^3\text{He}$  and heavy-ion abundances may be due to a mechanism wherein the  $^3\text{He}$  enrichment process operates only at coronal sites which happen to be enriched in heavy nuclei due to other reasons—and thus the  $^3\text{He}$  heating mechanism itself does not preferentially heat the heavy ions.

The observational techniques are described in § II, and the observations are presented in § III. Preliminary reports on parts of this work have been given elsewhere (Mason *et al.* 1984, 1985).

## II. INSTRUMENTATION AND EVENT SELECTION

The observations reported here were carried out in interplanetary space using sensors carried on the *ISEE 3* spacecraft. *ISEE 3* was launched on 1978 August 12 into a unique “halo orbit” about the sunward libration point  $\sim 240$  Earth radii away from Earth on the Earth-Sun line (Ogilvie, Durney, and von Rosenvinge 1978).

All the measurements of  $^3\text{He}$  and  $^4\text{He}$  reported here were taken with the two very low energy telescopes (VLETs) of the Goddard Space Flight Center cosmic ray experiment. The VLETs are solid state telescopes which identify particle type and energy using the  $dE/dx$  versus residual energy technique. The telescopes have an opening cone angle of  $50^\circ$  (full width) with excellent resolution of  $^3\text{He}$  and  $^4\text{He}$  (see Reames and von Rosenvinge 1981). Measurements of ions heavier than He reported here were performed with the ultra low energy wide angle telescope (ULEWAT) sensor, which was a portion of the Max-Planck-Institut/University of Maryland nucleonic and ionic charge distribution particle experiment. The ULEWAT is a multiple  $dE/dx$  versus residual energy telescope which employs flow-through proportional counters as the  $dE/dx$  elements. The use of proportional counters enables the simultaneous achievement of low-energy threshold and large geometrical factor, making this telescope ideal for studies of low-energy solar flare heavy ions. The ULEWAT has a rectangular field of view with opening angles of  $104^\circ$  by  $39^\circ$  where the larger angle is approximately bisected by the ecliptic plane. A complete description of the VLETs has been published by von Rosenvinge *et al.* (1978), and the ULEWAT has been described by Hovestadt *et al.* (1978).

Since the present study involves flux measurements from two different sensors, the question of intercalibration is important. Fluxes measured with the VLET and ULEWAT agreed well during diffusive solar flare or interplanetary events. However, during  $^3\text{He}$ -rich events, the fluxes did not agree well, with the ULEWAT He flux being a factor of  $\sim 2$  lower than the VLET measurements. The origin of this difference appar-

ently lies in the large anisotropies observed in these events for He (Reames and von Rosenvinge 1983; Reames, von Rosenvinge, and Lin 1985). This situation violates the assumption of isotropy used in calculating the telescope geometrical factors (e.g., Sullivan 1971). Such anisotropy would still yield agreement between the VLETs and ULEWAT if they sampled the same particle population; however, the ULEWAT has a much lower energy threshold than the VLETs, and therefore samples lower energy, more nearly isotropic protons simultaneously with the anisotropic helium. In the ULEWAT, this can lead to a “diluting” of the He flux by the low-energy proton flux, resulting in a lower calculated He flux than would be calculated using the VLET. Since the instruments do not transmit enough detailed information to identify unambiguously the relative roles of these type of flux differences, it was decided to intercompare the He flux levels as observed in 11  $^3\text{He}$ -rich events at the beginning of the survey period. This comparison led to an average measured ULEWAT helium flux level of 0.48 of the VLET reported value: it was then decided to apply this correction factor to the VLET fluxes when comparing them with the ULEWAT. Figure 1 shows the ratios of fluxes for the 11 events from the two instruments after this correction has been applied. The  $1\sigma$  spread around 1.0 derived from the scatter about the mean is 0.20; we thus conclude that this empirically derived correction factor yields agreement to within  $\sim 20\%$  between the two telescopes for the events in this study. It was not possible to extend the comparison shown in Figure 1 to periods beyond 1979 September, due to a decrease in the gain of the ULEWAT proportional counters which resulted in He signals falling beneath the instrument’s triggering threshold.

The  $^3\text{He}$ -rich events in this study were identified with the VLET in a search of the data from 1978 August 15 through 1982 June 30. Details of the search and selection criteria are given in Reames and von Rosenvinge (1983), and a list of key parameters of the 66 events has been published by Kahler *et al.* (1985b). Briefly, the data were scanned with 6 hr time resolution, and to be considered as a candidate event, the  $^3\text{He}/^4\text{He}$  ratio had to exceed 0.2 in two successive time periods. The energy intervals examined were 1.3–1.6 and 2.2–3.1 MeV per nucleon. Candidate events were then examined at higher time resolution in order to separate obvious multiple events

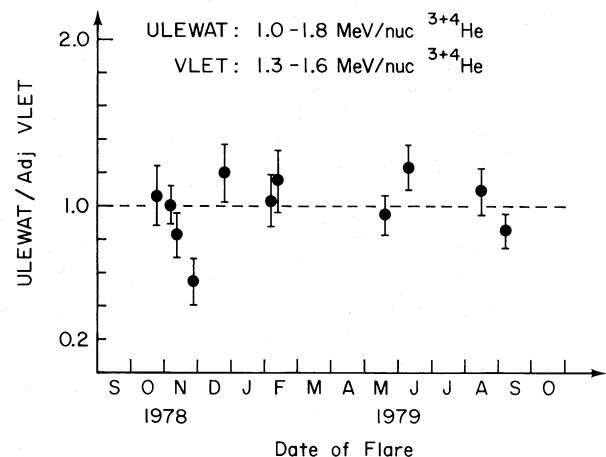


FIG. 1.—Intercomparison of flux measurements of the VLET and ULEWAT sensors in  $^3\text{He}$ -rich events, after adjustment for particle anisotropies.

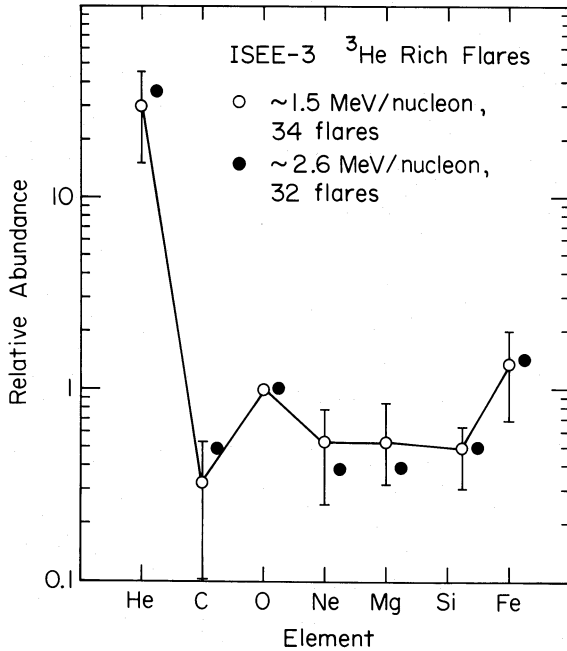


FIG. 2.—Abundances of the elements relative to oxygen in <sup>3</sup>He-rich events for two different energies. For He, the abundance shown is for <sup>4</sup>He only. Error bars on open points denote the range of values observed for two-thirds of the cases clustered around the mean values. Error bars on filled points are not shown to avoid crowding the figure.

and to identify the onset time. However, it is probable that some of these 66 periods contain unresolved multiple particle events. It is important to note that in only 35 of the 66 events were <sup>4</sup>He flux increases identified, and only 15 of the 66 events were accompanied by obvious proton events. Twelve (12) events showed both proton and <sup>4</sup>He flux increases (Kahler *et al.* 1985b). It should be pointed out that at the low energies of the particles discussed here, there are often rather high ambient flux levels of protons and <sup>4</sup>He in interplanetary space, due to, e.g., decays of large solar particle events, etc., and these ambient flux levels might mask modest H and <sup>4</sup>He flux increases associated with <sup>3</sup>He-rich events.

Spectral index data presented below for He and Fe were obtained by averaging the spectra over the entire <sup>3</sup>He-rich

event, and performing a weighted least-squares fit to the data assuming a power law in kinetic energy per nucleon  $dJ/dE \propto E^{-\gamma}$ . The minimum energy range covered was  $\sim 0.4$ – $1.6$  MeV per nucleon, with higher energy points used as available in those events with large fluences. Over the limited energy range investigated here, it was found that the spectra could in almost every case be adequately fitted by power laws in kinetic energy per nucleon.

### III. OBSERVATIONS

#### a) Relative Abundances

Figure 2 shows the abundances relative to oxygen calculated in an unweighted manner for all events for which there were observable increases in the <sup>4</sup>He flux, and a finite oxygen flux. Near 1.5 MeV per nucleon, 34 of the 66 events met these criteria, while 32 events were usable for measurements near 2.5 MeV per nucleon. In estimating the  $1\sigma$  widths of the abundance distributions, it is necessary to note that the measurements of abundances in individual events were *not* distributed in a Gaussian fashion around the mean values; rather, they were spread out much more widely. In order to represent the widths of the distributions in the data near 1.5 MeV per nucleon, we therefore show in Figure 2 the limit of values for two-thirds of the cases centered around the mean: i.e., the range of values covered with the extreme one-sixth of the distribution on both the high and low sides discarded. For the 2.5 MeV per nucleon point, these “ $1\sigma$ ” spreads are somewhat larger and are given in Table 1. Note that overall these “ $1\sigma$ ” limits are within plus or minus a factor of  $\sim 2$  about the mean for all species. Table 1 lists the average abundances and “ $1\sigma$ ” limits, as well as the entire range of relative abundances observed. The formal errors on the *mean* values of the abundances given in Table 1 are  $\sim \pm 10\%$ .

It can be seen from Figure 2 that the mean values of the relative abundances near 2.5 MeV per nucleon are well within the “ $1\sigma$ ” limits of the points near 1.5 MeV per nucleon. Thus over this rather limited energy range, we observe no dependence of the relative abundances on energy. From Figure 2 it is apparent that Fe is the *most abundant* of the heavy ions, and that the average <sup>4</sup>He/Fe ratio is greater than 20. Since the minimum <sup>3</sup>He/<sup>4</sup>He ratio accepted for inclusion in the survey was  $\sim 0.15$ , it should be noted that the <sup>3</sup>He flux *exceeds* the Fe

TABLE 1  
ABUNDANCE RATIOS IN <sup>3</sup>He-RICH SOLAR PARTICLE EVENTS

SPECIES	$\sim 1.5$ MeV PER NUCLEON <sup>b</sup>			$\sim 2.5$ MeV PER NUCLEON <sup>d</sup>		
	Abundance <sup>a</sup>	Limits of Two-thirds of cases <sup>c</sup>	Limits of All Cases	Abundance <sup>d</sup>	Limits of Two-thirds of cases <sup>c</sup>	Limits of All Cases
<sup>4</sup> He .....	30.1	15–45	6–122	35.8	12–52	0–142
C .....	0.33	0.10–0.53	0–1.50	0.49	0.18–0.85	0–2.03
O .....	1.	...	...	1.	...	...
Ne .....	0.54	0.25–0.78	0.10–1.50	0.38	0.16–0.70	0–0.96
Mg .....	0.53	0.32–0.84	0–1.23	0.39	0.14–0.52	0–1.11
Si .....	0.49	0.30–0.64	0.10–1.84	0.50	0.17–0.84	0–2.02
Fe .....	1.34	0.68–2.00	0.28–4.51	1.41	0.60–1.98	0–3.26

<sup>a</sup> Unweighted average of ratios with respect to oxygen for flares with measurable enhancements of <sup>4</sup>He over ambient levels.

<sup>b</sup> Energy range: <sup>4</sup>He, 1.34–1.63 MeV per nucleon, VLET; C–Fe, 1.0–1.8 MeV per nucleon, ULEWAT.

<sup>c</sup> 34 flares in survey.

<sup>d</sup> Energy range: <sup>4</sup>He, 2.29–3.03 MeV per nucleon, VLET; C–Fe, 1.8–3.4 MeV per nucleon, ULEWAT.

<sup>e</sup> 32 flares in survey.

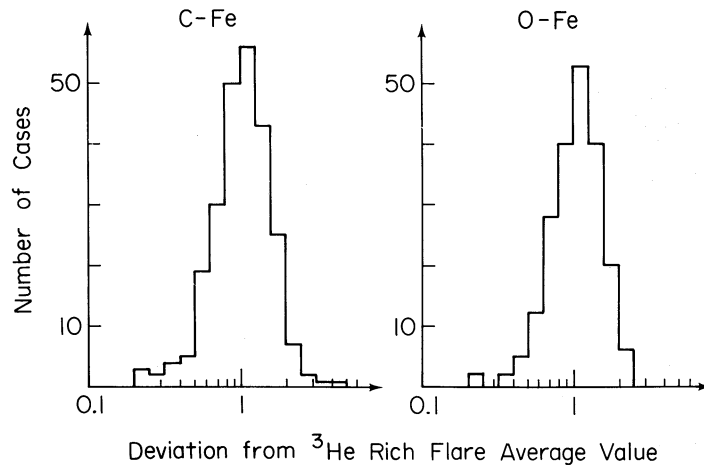


FIG. 3.—Deviations of individual element abundances in 42 events from a best fit to the average pattern (Fig. 2). *Left histogram*: deviations for fits over the element range C–Fe; *right histogram*: deviations for fits over the range O–Fe.

flux in these events. Examination of all 34 events yields a range from  $\sim 2$  to greater than 150 for the  $^3\text{He}/\text{Fe}$  ratio, with an average  $^3\text{He}/\text{Fe}$  value of  $\sim 30$ . Thus, the heavy ions are indeed the *minor* species in these events, with  $^3\text{He}$  almost always outnumbering the total number of heavy ions accelerated.

In view of the large range of  $^3\text{He}/^4\text{He}$  enrichments (from  $\sim 10^3$  to greater than  $10^4$  above coronal values) and, e.g., the range of a factor of greater than 80 for the  $^3\text{He}/\text{Fe}$  ratio reported here, one of the most surprising aspects of the heavy-nuclei relative abundances is the relatively narrow spread of values observed. The clustering of these values is displayed in Figure 3, which shows the histograms of the deviations from the  $^3\text{He}$ -rich event average values for the elements C–Fe and O–Fe near 1.5 MeV per nucleon. These histograms were constructed by comparing individual event abundances with the average abundances (Fig. 2 and Table 1) as follows: a single normalization value was found which minimized the weighted least-squares logarithmic deviation of an individual event's abundances from the average abundance for the range of elements C–Fe, and, separately, O–Fe. Taking this value of the normalization, the ratios between the renormalized event's abundances and the overall average abundances were calculated, and the values of these entered into the histogram with one value for each element. This procedure assures a histogram centered on unity, and the width of the histogram shows the degree to which individual elements deviate from the average pattern. In order to remove cases of poor statistical accuracy, only those events with relative abundance errors less than 0.8 were used: out of the total sample, 42 events met this test for elements with nonzero abundances.

The key feature of Figure 3 is the relative narrowness of the distributions: in the case of the range C–Fe, 90% of the points fall within a factor of 2 of the mean, that is in the range 0.5–2.0. Most of the more extreme deviations in the C–Fe histogram are due to the element carbon, as can be seen by comparing this histogram with the histogram covering the range O–Fe. For the O–Fe histogram, 93% of the points fall within a factor of 2 of the mean. While this factor of  $\sim 2$  spread in the range of heavy-ion abundances is larger than the spreads seen among large solar particle events (e.g., Mason *et al.* 1980), it is nevertheless very small compared to the range of  $^3\text{He}$  abundance variations and the range of the, e.g.,  $^3\text{He}/^4\text{He}$  ratio.

#### b) Enhancements Relative to Large Flares

The average abundances of the  $^3\text{He}$ -rich flares in the present survey are compared in Figure 4 and Table 2 with composition in large solar particle events and with previous work. For the data presented here we have normalized to the large-event abundances near 1 MeV per nucleon from Mason *et al.* (1980). Although the enhancements are normalized to unity at oxygen, this is an arbitrary choice, and it can be seen that there is an enrichment which increases with mass or atomic number over the whole range  $^4\text{He}$ –Fe. As a guide, the Fe/O ratio is enhanced by a factor of 10 compared with large events, and the  $\text{Fe}/^4\text{He}$  ratio is enhanced by a factor of  $\sim 20$ .

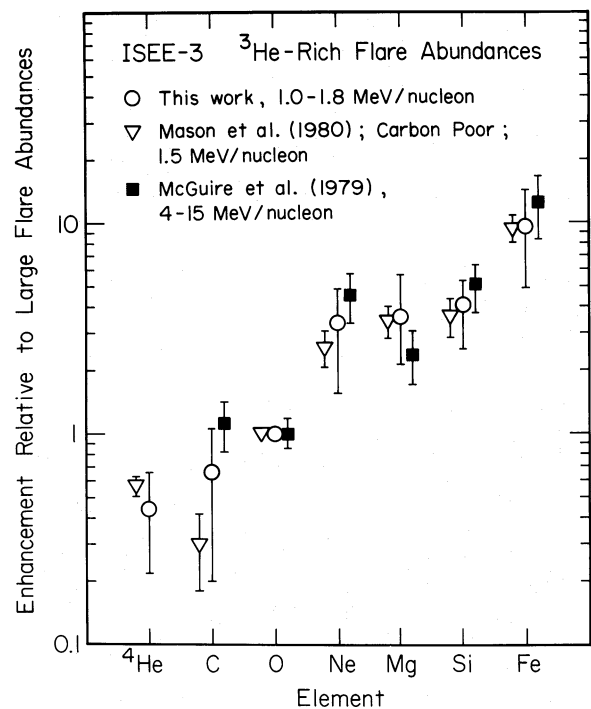


FIG. 4.—Enhancement of  $^3\text{He}$ -rich event element abundances compared to large solar particle event element abundances.

TABLE 2  
HEAVY-ION ENRICHMENTS IN  $^3\text{He}$ -RICH EVENTS RELATIVE  
TO LARGE-FLARE PARTICLE EVENT ABUNDANCES

SPECIES	1.5 MeV PER NUCLEON		2.5 MeV PER NUCLEON	
	Enrichment <sup>a</sup>	Limits of Two-thirds of Cases	Enrichment <sup>a</sup>	Limits of Two-thirds of Cases
$^4\text{He}$ .....	0.44	0.22– 0.66	0.53	0.18– 0.77
C .....	0.66	0.20– 1.06	0.98	0.36– 1.70
O .....	1.	...	1.	...
Ne .....	3.38	1.56– 4.88	2.38	1.00– 4.38
Mg .....	3.53	2.13– 5.60	2.60	0.93– 3.47
Si .....	4.08	2.50– 5.33	4.16	1.41– 7.00
Fe .....	9.57	4.86–14.29	10.07	4.29–14.14

<sup>a</sup> Relative to average large flare abundances near 1 MeV per nucleon (Mason *et al.* 1980).

It has been pointed out by several workers that for normal solar particle events, the ratio of the energetic particle to “local galactic” abundances shows a correlation with the first ionization potential (FIP) of the elements (e.g., Cook *et al.* 1979; McGuire, von Roseninge, and McDonald 1979a; Mewaldt 1980; Breneman and Stone 1985; Meyer 1985). It is found that low first ionization potential elements such as Mg, Si, and Fe are enhanced by a factor of  $\sim 3$ –4 with respect to high first ionization potential elements such as O, Ne, and He. The abundance pattern shown here in Figure 4 for  $^3\text{He}$ -rich events does not appear to fit into this FIP pattern, since for the two elements with highest first ionization potential (He and Ne), one shows a *decrease* from normal flare abundances by a factor of more than 2, and the other shows an *increase* by a factor of  $\sim 3$ . This destroys the pattern seen in plots using normal flare energetic particle abundances, since in the  $^3\text{He}$ -rich events the element Ne is overabundant even though it has a high first ionization potential. We conclude that the enrichment pattern seen in  $^3\text{He}$ -rich events, compared to large solar particle event abundances, is not a more extreme version of the FIP pattern, but is rather distinct and therefore must be due to other processes than those responsible for the FIP pattern.

Figure 4 also shows enrichments near 1 MeV per nucleon for three “carbon-poor” flares which occurred in 1974 as reported by Mason *et al.* (1980). The data from McGuire, von Roseninge, and McDonald (1979b) cover the energy range 4–15 MeV per nucleon, and are based on a survey of 17  $^3\text{He}$ -rich events observed during 1974–1978 (three of these 17 events are among the 66 flares in the present survey). In the enrichments from McGuire, von Roseninge, and McDonald (1979b), the “normal flare” reference composition is from flare events “not enhanced in Fe”; nevertheless, these higher energy observations are in good agreement with the more extensive survey presented here.

In Figure 4 we note that the stated errors from the earlier work are the uncertainty in the *mean* of the distribution, and therefore are smaller than the “ $1\sigma$ ” limits (i.e., the width of the distributions) shown in the present work. The  $1\sigma$  limits used here give a better idea of the range of values observed over a number of events. Given the fact that the earlier results for heavy-ion enrichments shown in Figure 4 are based almost completely on an independent set of events from the present work, the close agreement with the present work reinforces our earlier conclusion that the heavy-ion abundance pattern is remarkably constant from one  $^3\text{He}$ -rich event to another. In

addition, the close agreement between the present results near 1.5 MeV per nucleon and the considerably higher energy observations of McGuire, von Roseninge, and McDonald (1979b) extends and significantly strengthens the earlier cited evidence (Fig. 2) that there is no appreciable energy dependence to the abundance pattern.

### c) Search for Correlations among Measured Quantities

#### i) Flux Level Correlations

In order to see if any pairs of ion fluxes showed unusual correlations, correlation coefficients for logarithms of the weighted flux levels among all the species in the survey were calculated and are given in Table 3. For a flux level in a particular event to be used in the calculation for this table, a fractional error of less than 0.8 was required, and, in the case of  $^3\text{He}$  and  $^4\text{He}$  fluxes, it was required that the  $^4\text{He}$  flux show an increase over ambient levels. With these criteria, between 20 and 30 flux values were available for calculating each correlation coefficient. Because fluxes always increase together in the events, the correlation coefficients are all quite high, covering the range 0.62–0.93. Even for the points with the lowest correlation coefficients, the probability that there is no correlation between the quantities is less than 0.001. Note that the  $^3\text{He}$ : $^4\text{He}$  correlation coefficient is not as large as many other values in the table, particularly among the heavy ions. The correlations with Fe are strongest for Ne, Mg, and Si, and are rather less with the lighter elements. Overall there is a trend for elements to be most strongly correlated with those of nearby atomic mass or atomic number similar to the case with large flare particle events (Mason *et al.* 1980). However, no pair of elements stands out from the group by showing dramatically higher correlations than other pairs.

#### ii) Enrichments versus Spectral Index

Differing acceleration processes may produce particle energy spectra with distinctive shapes (e.g., review by Forman, Ramaty, and Zweibel 1985), which might be usable to help discern properties of the acceleration mechanism. For example, in large particle events the strong correlation of the electron: proton ratio and the electron spectral index (Evenson *et al.* 1984) may be a signature of shock wave acceleration (Lin, Mewaldt, and Van Hollebeke 1982; Ellison and Ramaty 1985). In the case of  $^3\text{He}$ -rich events, Möbius *et al.* (1982) have proposed a stochastic Fermi acceleration mechanism in which the calculated energy spectra depend on the power-law index  $n$  of the magnetic irregularity spectrum at the acceleration site. In this model the energy dependence of the  $^3\text{He}/^4\text{He}$  ratio and the Fe/O ratio depend on  $n$ , with smaller values of  $n$  producing steeper energy dependences. Thus, spectral forms or energy

TABLE 3  
 $^3\text{He}$ -RICH EVENTS: CORRELATION COEFFICIENTS BETWEEN  $\ln(\text{fluxes})$

ELEMENT	COEFFICIENT VALUE							
	$^3\text{He}$	$^4\text{He}$	C	O	Ne	Mg	Si	Fe
$^3\text{He}$ .....	1.	0.813	0.759	0.781	0.622	0.709	0.810	0.639
$^4\text{He}$ .....		1.	0.846	0.867	0.694	0.748	0.810	0.667
C .....			1.	0.836	0.685	0.718	0.795	0.645
O .....				1.	0.870	0.903	0.905	0.882
Ne .....					1.	0.917	0.864	0.917
Mg .....						1.	0.924	0.930
Si .....							1.	0.916
Fe .....								1.

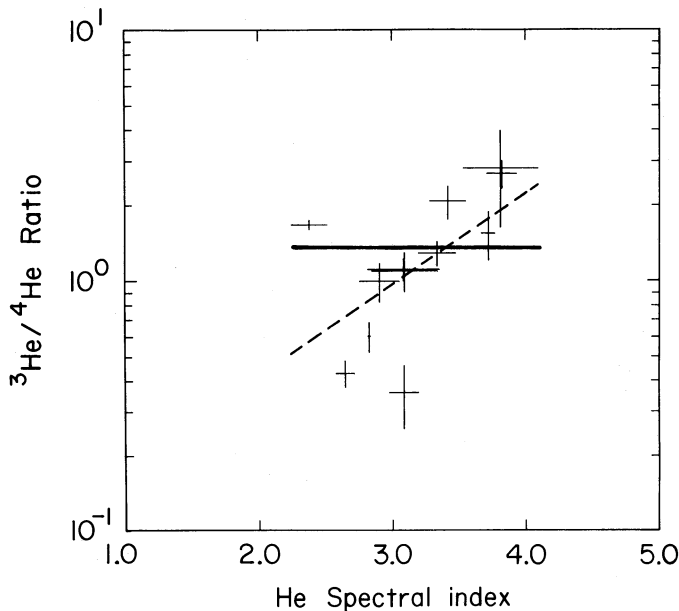


FIG. 5.—VLET  ${}^3\text{He}/{}^4\text{He}$  ratio vs. the ULEWAT  ${}^3\text{He} + {}^4\text{He}$  spectral index, assuming a power law in kinetic energy per nucleon. *Dark line*: weighted least-squares fit to the data. *Dashed line*: unweighted fit.

dependences of the relative abundances (or lack of such dependences) constrain possible models for the acceleration.

Figure 5 shows the  ${}^3\text{He}/{}^4\text{He}$  ratio plotted versus  ${}^3\text{He} + {}^4\text{He}$  spectral index for those events observed with the ULEWAT in the period before the instrument's sensitivity to helium decreased. The weighted least-squares fit (*dark line*) in the figure is consistent with no correlation (slope  $-0.02 \pm 0.18$ ), while *unweighted* fit (*dashed line*) shows a significant positive correlation (slope  $2.5 \pm 1.2$ ). Inspection of Figure 5 shows that a single event (1979 December 14) with low spectral index and high  ${}^3\text{He}/{}^4\text{He}$  ratio is responsible for most of the difference between the two fits. In view of the relatively small number of events and the relatively narrow energy range over which the He spectral index is measured, it is clear that further investigations would be necessary in order to establish the degree of correlation between the  ${}^3\text{He}/{}^4\text{He}$  ratio and spectral index. A positive correlation between these quantities might also be inferred from the data of Reames and von Roseninge (1983).

Figure 6 shows a correlation plot for the Fe/O ratio versus the Fe spectral index for 48 flares in the survey. The slope of the least-squares fit line shown in the figure is  $-0.27 \pm 0.28$ , and is thus consistent with no correlation. It should be pointed out that the lack of correlation of Fe/O ratio with spectral index, along with the previously shown energy independence of the abundance enhancement pattern, suggests that the enrichments are due to abundance patterns in the injected material, rather than a result of the final step of the acceleration mechanism which energizes the particles to MeV energies.

#### iii) C/O and Fe/O Enhancements versus ${}^3\text{He}/{}^4\text{He}$ Ratio

It has been shown above that, compared with the large-flare event composition,  ${}^3\text{He}$ -rich events as a group have a distinctive enrichment pattern for heavy ions. In order to examine whether these enrichments correlate in detail with the  ${}^3\text{He}$  enrichments, Figure 7 shows the C/O ratio versus  ${}^3\text{He}/{}^4\text{He}$  ratio, and Figure 8 shows the Fe/O ratio plotted versus  ${}^3\text{He}/{}^4\text{He}$ . For these plots the ratios were used only if they had

relative errors less than 0.8, and only if there was an increase of  ${}^4\text{He}$  fluxes over ambient levels for the event. In the case of the C/O ratio, note that in some flares there is a very small value (i.e., carbon-poor flares), but these depletions do *not* correlate with the  ${}^3\text{He}/{}^4\text{He}$  ratio. The slope of the least-squares fit line of  $0.07 \pm 0.09$  is consistent with no correlation.

The Fe/O ratio plot in Figure 8 might be expected to show the greatest sensitivity to the  ${}^3\text{He}/{}^4\text{He}$  ratio, since this ratio is enhanced by a large amount in  ${}^3\text{He}$ -rich events compared to large solar particle events. Yet there is no statistically significant correlation (least-squares fit line slope is  $0.02 \pm 0.06$ ). Notice however, that the Fe/O ratio is sufficiently enhanced in these events that even the lowest value shown in the figure is still well in excess of the range of values of Fe/O seen in large flares (Mason *et al.* 1980). Table 4 shows the composition of all elements for each event included in Figure 8.

#### iv) Fe/O Enhancements in Proton Events

As mentioned previously, 12 of the 66 events in this survey showed proton and  ${}^4\text{He}$  flux increases over ambient levels. Kahler *et al.* (1985b) have shown that for the same set of events, those 12 with proton and  ${}^4\text{He}$  flux increases showed a lower  ${}^3\text{He}/{}^4\text{He}$  ratio (0.42) than the average  ${}^3\text{He}/{}^4\text{He}$  ratio (0.76) for the 35 events which showed  ${}^4\text{He}$  increases. This difference was interpreted as being due to an admixture of "normal" particle event material in the proton events which tended to reduce the  ${}^3\text{He}/{}^4\text{He}$  ratio (Kahler *et al.* 1985b). We do not observe such an effect for the heavy-ion abundances: for the 12 proton events,  $\text{Fe}/\text{O} = 1.7 \pm 0.9$ , while for the events with  ${}^4\text{He}$  increases  $\text{Fe}/\text{O} = 1.3 \pm 0.7$ , where the uncertainties are the "1  $\sigma$ " limits as discussed above. Thus, the Fe enhancement characteristic of  ${}^3\text{He}$ -rich events is not decreased to lower values by "normal" flare event material in proton events.

#### d) Deviations from ${}^3\text{He}$ -rich Event Average Abundances

Having described the average properties of heavy-ion abundances in previous sections, we now turn to cases of extreme deviations from the average in order to see if there are any additional, unusual properties which might yield further infor-

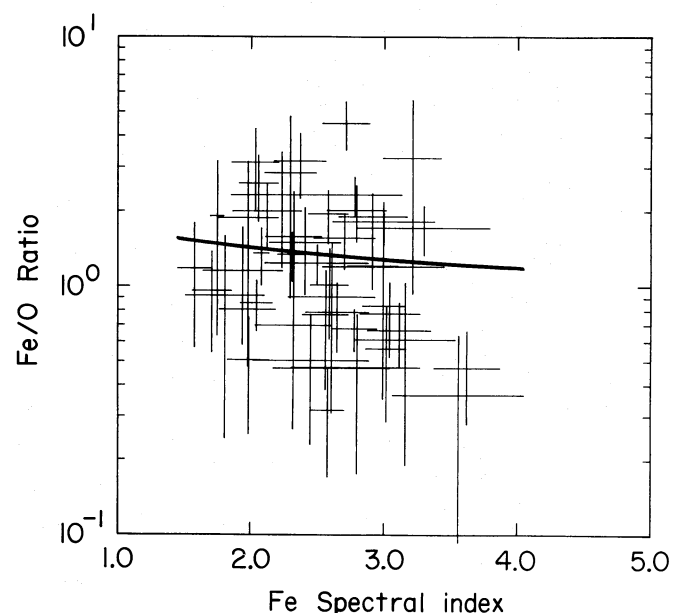
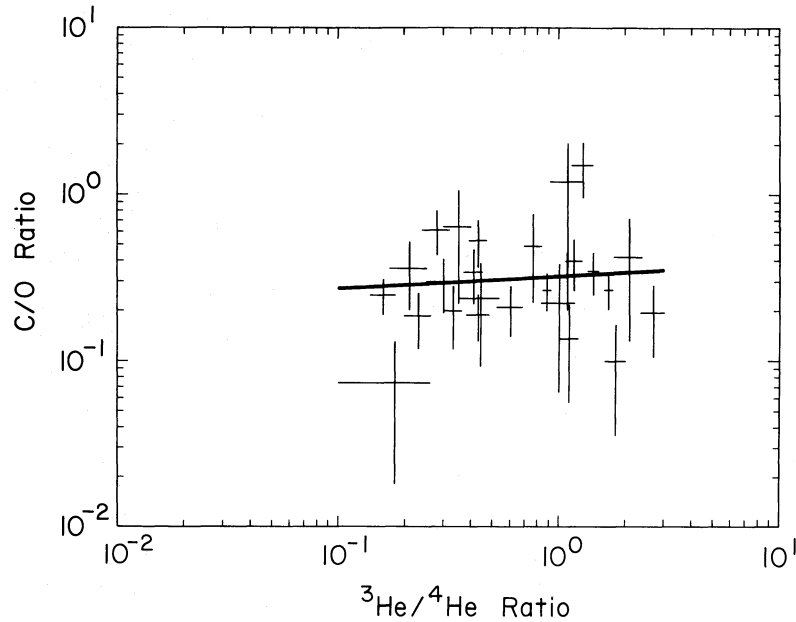


FIG. 6.—Fe/O ratio (1.0–1.8 MeV per nucleon) vs. Fe spectral index

FIG. 7.—C/O ratio vs.  $^3\text{He}/^4\text{He}$  ratio

mation on the acceleration mechanism. In searching for events with abundance patterns significantly different from average, we must note that with some 66 reference events with several species measured in each, there are altogether several hundred individual abundance points, and so a few cases of extreme variations would be expected from statistical fluctuations alone. To identify candidate events, a least-squares fit was done between the average abundance values (Fig. 2 and Table 1) and the abundances in each event. The reduced  $\chi^2$  from these fits for the elements O–Fe are shown in Figure 9 along with the distribution of reduced  $\chi^2$  expected from random fluctuations alone (line labeled “calculated” in the figure). It may be seen from the figure that the distribution of reduced  $\chi^2$  follows the

calculated pattern rather well, except that there were eight cases with  $\chi^2 > 3$ , versus only about one case expected from random fluctuations. A similar set of fits for the range C–Fe identified 10 events with  $\chi^2 > 3$  versus one expected; these events included all the cases identified in the O–Fe fits except one, for a total of 11 separate events with  $\chi^2 > 3$  for the heavy-ion fits to the average abundances. Before examining these cases in more detail, we point out that the distribution of  $\chi^2$  when comparing the present set of events with large solar particle event abundances produces generally very poor results (*open circles*, Fig. 9) with almost  $\frac{2}{3}$  of the cases producing  $\chi^2 > 3$ . This comparison can be taken as an indication of the statistical accuracy of the heavy-ion data in this survey: in

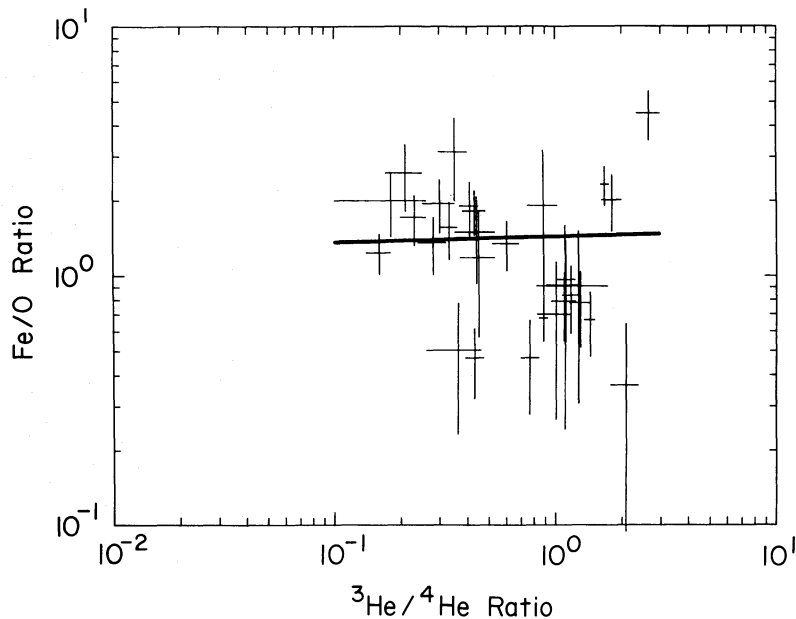
FIG. 8.—Fe/O ratio vs.  $^3\text{He}/^4\text{He}$  ratio. Table 4 lists the abundances for other species for all the events whose Fe/O ratio is in this figure.

TABLE 4  
ABUNDANCES IN SELECTED  $^3\text{He}$ -RICH SOLAR PARTICLE EVENTS

$^3\text{He}$ ONSET DATE	TIME (UT)	DURATION (hr)	$^3\text{He}/^4\text{He}$ RATIO <sup>a</sup>	ABUNDANCES RELATIVE TO OXYGEN <sup>b</sup>					
				C	O	Ne	Mg	Si	Fe
1978 Oct 23	16:00	24	1.10 ± 0.19	1.19 ± 0.83	1.	0.62 ± 0.49	0.96 ± 0.73	0.17 ± 0.19	0.92 ± 0.67
Nov 3	8:00	28	1.29 ± 0.14	1.50 ± 0.54	1.	0.28 ± 0.13	0.84 ± 0.33	0.40 ± 0.17	0.78 ± 0.26
Nov 8	22:00	24	0.36 ± 0.10	0.	1.	0.53 ± 0.30	0.82 ± 0.40	0.24 ± 0.17	0.50 ± 0.27
Dec 26	16:00	20	2.07 ± 0.30	0.42 ± 0.29	1.	0.09 ± 0.10	0.41 ± 0.30	0.94 ± 0.56	0.37 ± 0.27
1979 Feb 6	2:00	72	1.00 ± 0.17	0.22 ± 0.16	1.	0.52 ± 0.34	0.55 ± 0.38	0.17 ± 0.13	0.70 ± 0.43
Feb 10	5:00	48	1.11 ± 0.11	0.14 ± 0.08	1.	0.24 ± 0.12	0.32 ± 0.13	0.40 ± 0.20	0.96 ± 0.42
Sep 6	14:00	44	0.43 ± 0.05	0.19 ± 0.06	1.	0.51 ± 0.13	0.40 ± 0.11	0.37 ± 0.10	1.82 ± 0.37
Oct 3	16:00	40	0.60 ± 0.08	0.21 ± 0.07	1.	0.47 ± 0.13	0.41 ± 0.12	0.40 ± 0.11	1.35 ± 0.30
Dec 14	12:00	36	1.67 ± 0.07	0.27 ± 0.06	1.	0.24 ± 0.06	0.47 ± 0.10	0.64 ± 0.13	2.33 ± 0.41
Dec 23	11:00	48	2.67 ± 0.33	0.19 ± 0.09	1.	0.94 ± 0.26	1.08 ± 0.28	0.97 ± 0.27	4.51 ± 1.00
1980 Jan 13	24:00	32	1.80 ± 0.18	0.10 ± 0.06	1.	0.88 ± 0.26	0.90 ± 0.26	0.65 ± 0.20	2.02 ± 0.51
Feb 13	20:00	12	1.09 ± 0.14	0.33 ± 0.13	1.	0.53 ± 0.18	0.26 ± 0.10	0.27 ± 0.11	0.79 ± 0.24
Mar 16	10:00	32	1.27 ± 0.45	0.04 ± 0.05	1.	0.25 ± 0.22	0.41 ± 0.36	0.62 ± 0.47	0.91 ± 0.60
Mar 25	15:00	24	0.44 ± 0.09	0.24 ± 0.14	1.	0.78 ± 0.36	0.50 ± 0.28	0.34 ± 0.16	1.50 ± 0.57
Mar 30	14:00	16	0.76 ± 0.07	0.49 ± 0.26	1.	0.18 ± 0.09	0.23 ± 0.11	0.26 ± 0.12	0.47 ± 0.19
Apr 13	13:00	8	0.18 ± 0.08	0.07 ± 0.06	1.	0.54 ± 0.20	0.62 ± 0.22	0.42 ± 0.17	2.00 ± 0.57
Jun 23	6:00	18	0.43 ± 0.04	0.53 ± 0.17	1.	0.17 ± 0.07	0.26 ± 0.09	0.34 ± 0.12	0.47 ± 0.15
Jun 28	2:00	28	0.21 ± 0.04	0.36 ± 0.16	1.	0.76 ± 0.27	0.83 ± 0.29	0.46 ± 0.19	2.59 ± 0.77
Jun 29	16:00	18	0.35 ± 0.05	0.64 ± 0.42	1.	0.70 ± 0.29	0.37 ± 0.17	0.54 ± 0.24	3.14 ± 1.15
Jul 9	2:00	12	0.30 ± 0.05	0.30 ± 0.11	1.	0.75 ± 0.21	0.58 ± 0.17	0.52 ± 0.16	1.95 ± 0.47
Nov 9	17:00	20	1.43 ± 0.08	0.35 ± 0.10	1.	0.11 ± 0.04	0.36 ± 0.12	0.30 ± 0.09	0.67 ± 0.19
Dec 16	19:00	16	0.45 ± 0.08	0.	1.	0.50 ± 0.32	0.14 ± 0.12	0.10 ± 0.10	1.18 ± 0.61
1981 Mar 23	8:00	36	0.28 ± 0.04	0.61 ± 0.18	1.	0.47 ± 0.14	0.58 ± 0.17	0.59 ± 0.20	1.36 ± 0.35
Jul 31	4:00	24	0.33 ± 0.03	0.20 ± 0.08	1.	0.42 ± 0.14	0.47 ± 0.16	0.48 ± 0.16	1.56 ± 0.40
Sep 15	22:00	36	1.17 ± 0.10	0.40 ± 0.13	1.	0.38 ± 0.15	0.27 ± 0.10	0.43 ± 0.16	0.83 ± 0.25
Nov 20	13:30	36	0.16 ± 0.02	0.25 ± 0.06	1.	0.39 ± 0.08	0.35 ± 0.08	0.38 ± 0.08	1.24 ± 0.22
1982 Mar 10	16:00	28	0.88 ± 0.04	0.27 ± 0.07	1.	0.22 ± 0.05	0.32 ± 0.07	0.54 ± 0.12	0.68 ± 0.13
Jun 25	8:00	12	0.23 ± 0.03	0.19 ± 0.07	1.	0.30 ± 0.10	0.48 ± 0.14	0.39 ± 0.11	1.71 ± 0.39
Jun 25	23:00	12	0.41 ± 0.04	0.34 ± 0.12	1.	0.76 ± 0.21	0.79 ± 0.23	0.43 ± 0.14	1.90 ± 0.46
Jun 30	13:00	12	0.88 ± 0.14	0.84 ± 0.68	1.	1.09 ± 0.86	1.03 ± 0.82	0.46 ± 0.51	1.91 ± 1.27

<sup>a</sup> Helium energy range: 1.3–1.6 MeV per nucleon.

<sup>b</sup> C, O, Ne, Mg, Fe energy range: 1.0–1.8 MeV per nucleon.

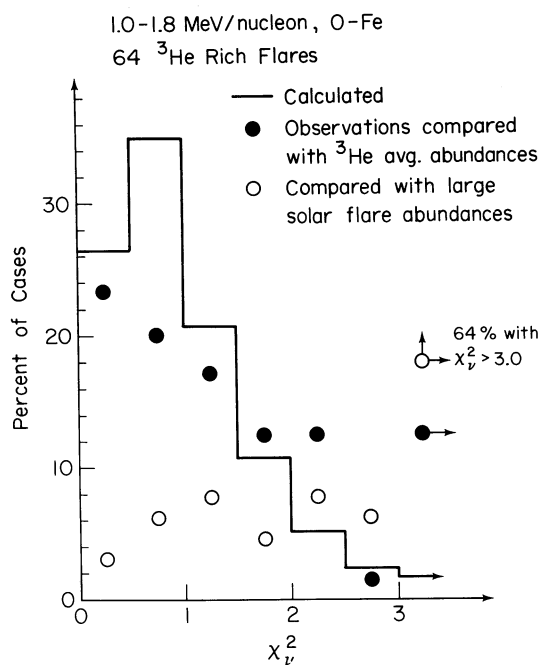


FIG. 9.—Distribution of reduced  $\chi^2$  for 64  $^3\text{He}$ -rich event heavy-ion abundances compared with (filled circle, ●)  $^3\text{He}$ -rich event set average abundances, and (open circle, ○), large solar flare event abundances

about two-thirds of the cases the accuracy is great enough to clearly distinguish between these events and large solar particle event abundances.

Inspection of the previously cited 11 events with  $\chi^2 > 3$  made it immediately clear that the most intense events, whose abundances are measured with the greatest statistical precision, would tend to produce large  $\chi^2$  values even for very small deviations from the  $^3\text{He}$ -rich event average values. It was found that seven of these 11 events had abundances which fell within the “1  $\sigma$ ” range of values shown in Figure 2, and therefore could not be really considered anomalous. The remaining four cases are shown in Figure 10, where we plot the individual flare enrichment versus large events and show also the “1  $\sigma$ ” range of values for  $^3\text{He}$ -rich events. In terms of  $^3\text{He}$  fluence, these events were not especially large: 1978 November 3 was 16th in  $^3\text{He}$  fluence out of 66; 1979 December 23 was seventh; 1980 November 9 was third; and 1982 March 18 was 33rd.

Considering case (a), 1978 November 3, it is apparent that the range O–Fe is consistent with the pattern found in  $^3\text{He}$ -rich events, while carbon is enriched by about 3 standard deviations. The probability of such a positive deviation is  $\sim 0.2\%$ , and could be expected once among  $\sim 500$  samples. In view of the large number of element abundances tested (64 events with six elements per event, for a total of 384 cases), a single such deviation might not be too surprising. Case (b), 1979 December 23, shows a pattern that appears to be merely a somewhat more extreme case of the average enrichment pattern observed

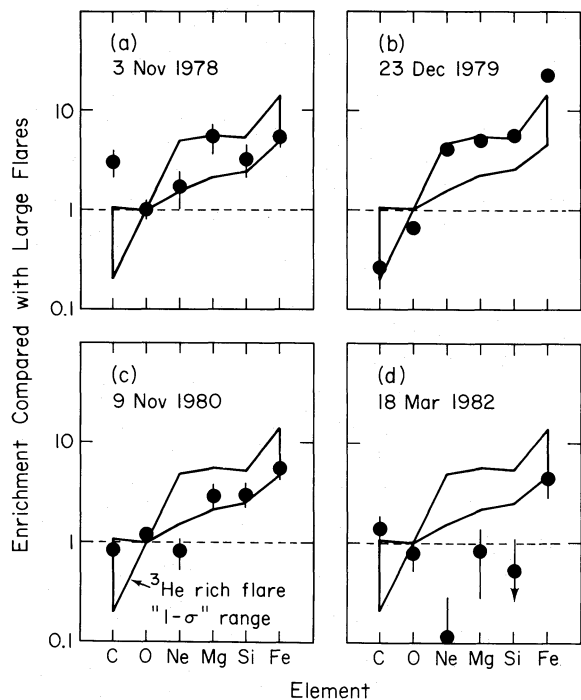


FIG. 10.—Enhancements with respect to large solar particle event abundances of  $^3\text{He}$ -rich events with unusual heavy-ion abundance patterns

in  $^3\text{He}$ -rich events. This event has also been discussed by Reames and von Roseninge (1981). Case (c), 1980 November 9, shows a range of elements (C–Ne) with relative abundances typical of large solar particle events, while heavier elements are consistent with the  $^3\text{He}$  enrichment pattern. Case (d), 1982 March 18, shows normal particle event abundances except for Fe, which is moderately enriched. The limited “range” of enrichments for case (c) and (d) are similar to those reported by Mason *et al.* (1980) for the 1977 October 12–13  $^3\text{He}$ -rich event, where only the elements Si–Fe appeared to be enriched compared with large solar particle event abundances.

#### e) Summary of Observations

Based on our survey of the low-energy heavy-ion abundances in a set of 66  $^3\text{He}$ -rich events, the major observational findings are the following:

1. There exists a characteristic abundance pattern (within a factor of  $\sim 2$ ) wherein heavy ions C, O, Ne, Mg, Si, Fe are enriched compared to large solar flare abundances; for example, Fe/O is enriched by a factor of  $\sim 10$ , and Fe/ $^4\text{He}$  is enriched by a factor of  $\sim 20$ .

2. This enrichment of heavy ions:
  - i) Increases with atomic mass and/or atomic number, but
  - ii) Does *not* correlate well with first ionization potential;
  - iii) Is energy independent;
  - iv) Is independent of spectral exponent;
  - v) Is independent of the  $^3\text{He}/^4\text{He}$  ratio.

3. The heavy-ion abundances tend to be well correlated with each other and show a smaller range of relative values than the  $^3\text{He}/^4\text{He}$  ratio.

4. Although heavy ions are enriched in these events, the average  $^3\text{He}/\text{Fe}$  ratio is  $\sim 30$ , with a range from  $\sim 2$  to greater than 150; thus,  $^3\text{He}$  is much more abundant than heavy ions in these events.

5. Deviations from the  $^3\text{He}$ -rich event average heavy-ion abundance pattern are rare, with two cases out of 66 exhibiting an apparent mixing of normal particle event and  $^3\text{He}$ -rich event abundance patterns.

#### IV. COMPARISON OF HEAVY-ION ENRICHMENTS WITH MODEL CALCULATIONS

The present study has confirmed and significantly extended previous work concerning the association between  $^3\text{He}$  enrichments and heavy-nuclei enrichments in solar particle events. This association, along with the lack of  $^2\text{H}$  and  $^3\text{H}$  in these events, has been generally accepted as indicating that proposed  $^3\text{He}$  enrichment mechanisms depending on spallation reactions or thermonuclear reactions are unable to explain the full range of observed characteristics of these events (e.g., Ramaty *et al.* 1980; Kocharov and Kocharov 1984). We now consider other suggested models for  $^3\text{He}$ -rich flares in order to compare their predictions with the new results presented here. It must be emphasized that all these models are two-stage models in which the first step involves preferential heating of the plasma followed by a second step in which those ions above some, e.g., velocity or rigidity threshold are energized to the  $\sim \text{MeV}$  energies observed in interplanetary space. Based on the similarity of the particle energy spectra leading to the overall lack of energy dependence of the relative abundances (e.g. § III), it is assumed that the enrichments are due to plasma abundances after the first step heating mechanism, with the second stage merely energizing the particles without introducing additional significant distortions. Below we therefore discuss only the abundances in the plasma after the first stage, taking for granted the operation of the second stage.

##### a) Plasma Resonance Models

The only theoretical papers with explicit predictions for heavy-ion enrichments in  $^3\text{He}$ -rich events are by Kocharov and Orishchenko (1983, 1985). Their model uses stochastic acceleration by Langmuir or ion-sound waves, and is an outgrowth of work by Ibragimov and Kocharov (1977) and Kocharov and Kocharov (1981). Figure 11a compares the heavy-ion abundance pattern reported here to the pattern from Kocharov and Orishchenko (1983) for two different time limits of heating in their model. While there is a general similarity between the model predictions and observations, the agreement is not particularly good. A revised model (Kocharov and Orishchenko 1985) produces a better fit for the element Si, but overestimates the Fe enrichment to the same degree as shown in Figure 11a. In their papers Kocharov and Orishchenko compare their model with single events only (the 1974 May 7–13 period in one case, and the  $^3\text{He}$ -poor flare of 1977 September 24 in the other), and it is possible that another selection of model parameters would yield better agreement with the average data presented here. As mentioned earlier, Weatherall (1984) has questioned the calculations of the series of papers by Kocharov and collaborators, and so their model must be considered controversial.

Another plasma resonance mechanism, proposed by Fisk (1978), enriches  $^3\text{He}$  by preferential heating via electrostatic ion-cyclotron waves (see also Varvoglis and Papadopoulos 1983). The Fisk model is only a preheating model, and it explicitly assumes an additional mechanism which takes the heated material above some velocity threshold and accelerates it to higher energies. Fisk (1978) pointed out that the  $^3\text{He}$  enrichment mechanism in this model might also preferentially

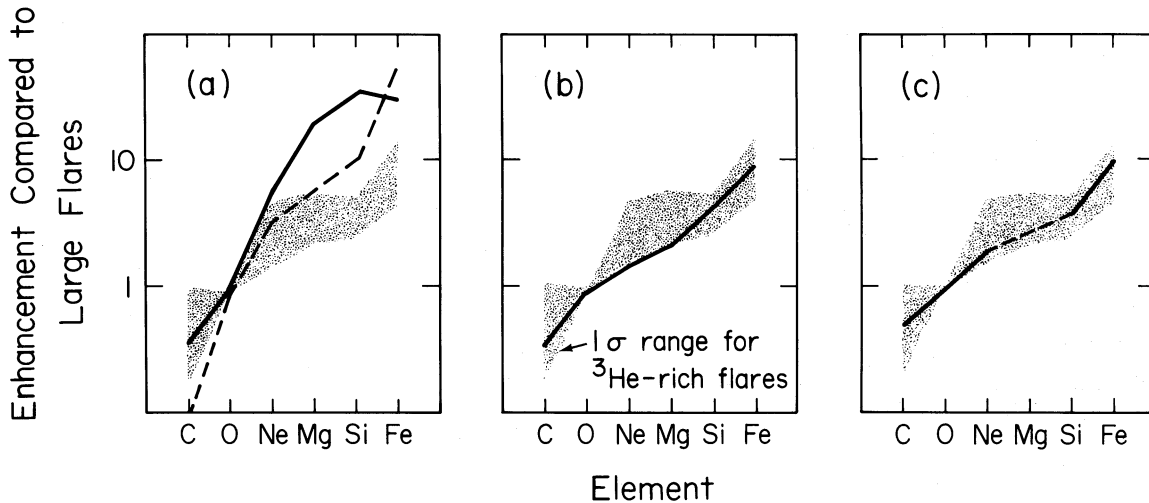


FIG. 11.— $^3\text{He}$ -rich event enrichment pattern compared to (a) model of Kocharov and Orishchenko (1983) for short heating time limit (solid line) and long heating time limit (dashed line); (b) “Fisk” plasma heating model with  $\omega_{\text{low}} = 1.0$ , temperature  $T$  range of  $10^4$ – $10^7$  K, and plasma volume elements  $\propto T^{0.5}$ . (c) Nakada (1969) lower coronal heavy-ion abundance enhancements.

heat heavy ions, since they can have the second harmonics of their gyrofrequency in the range of the ion-cyclotron wave frequencies. Mason *et al.* (1980) showed that for this mechanism to operate for a range of heavy-ion species, a range of temperatures was required since at no single temperature were all the heavy ions in the proper ionization states. However, no specific predictions have been made for heavy nucleus enrichments with this model, other than a qualitative noting that the element carbon might be greatly depleted compared to heavier nuclei (Fisk 1979; Mason *et al.* 1980).

In order to examine the specific predictions that might arise from the Fisk model we have calculated the *fractions* of material that are in the proper ionization state for resonant heating under various assumed coronal conditions. By normalizing the resonantly heated fractions of each element isotope to the comparable fraction of oxygen we have a set of values for preferentially heated abundances relative to oxygen. Presumably this set of values is also the observed enrichment compared with large solar flares, since it is assumed that the “normal” flare composition arises from an ambient coronal population. For example, if the fraction of Fe in the proper ionization state for resonant heating was *twice* the fraction of O that was in the proper ionization state, then in this simple model the Fe/O ratio would be *twice* the normal values for large flares. The isotopic abundances of the coronal material were taken from solar system abundances of Anders and Ebihara (1982), and element ionization states as a function of temperature were from Shull and Van Steenberg (1982).<sup>2</sup>

In order to complete the calculation for this simplified model, it is necessary to specify also (a) the range of temperatures in the plasma, (b) the lower bound of the electrostatic ion-cyclotron wave frequencies, and (c) the *volumes* of plasma at each temperature. For the temperature range, it was decided to span a broad range from  $10^4$ – $10^7$  K in order to cover the full range of temperatures required for each element in our survey to have the proper ionization state (although, of course, any

single element would have the favored ionization state(s) over a small portion of this range). Such a broad range of temperatures might arise from Joule heating of the plasma during the preheating process (Mason *et al.* 1980), or it could reflect the differing volumes of material having different temperatures. For example, in cool loops over sunspots a broad range of temperatures is observed (e.g., Foukal 1976). In the case of specifying the wave frequencies, the lower bound of the second harmonic of the waves was kept near the typical value of 1.05, while the upper bound was taken as  $2\Omega_i/\Omega_{\text{He}} \lesssim 1.19 + 0.13 (m_{\text{He}}/m_i)^{1/2}$ , where  $\Omega_i$  and  $\Omega_{\text{He}}$  are the cyclotron frequency of the ion and  $^4\text{He}$ , respectively, and  $m_{\text{He}}$  and  $m_i$  are the atomic masses (see Mason *et al.* 1980, eq. [6]).

Figure 11b compares the heavy-ion element enhancements reported here with the results of the simplified “Fisk” model for parameters specified in the figure caption. A slightly low value of  $\omega_{\text{low}}$  of 1.0 was used in order to improve the fit for carbon: using the nominal value of  $\omega_{\text{low}} = 1.05$  produced a C/O ratio of 0.2, somewhat lower than the observations. The dependence of volume elements on temperature  $T$  was chosen in order to optimize the fit for Fe enrichments: increasing the volume of plasma at the higher temperatures increases the Fe enrichment to values above the observations. For example, selecting volume  $\propto T^1$  predicts an Fe/O enhancement of 30:1 versus our observed enhancement of  $\sim 10$ :1. While the agreement between the observations and this “Fisk” enhancement model for the case plotted in Figure 11b is not unacceptable, we note that is has been achieved only through the use of several parameters, and it is not at all clear why these particular parameters would appear with such regularity in a large number of  $^3\text{He}$ -rich events. Seemingly minor variations of these parameters (e.g.,  $\omega_{\text{low}}$  or the volume-temperature relation) produce patterns markedly different from the average result observed in our survey. We note also that the feature of essentially the same enrichment (vs. oxygen) for Ne, Mg, Si seen in our observations is not reproduced in this model nor in the Kocharov plasma heating model.

#### b) Coulomb Friction Model

Another possible explanation for the heavy-element enrichments observed in  $^3\text{He}$ -rich events is that their heavy-element

<sup>2</sup> In the range of a few times  $10^6$  K the tables of Jordan (1969) show higher Fe ionization states than Shull and Van Steenberg (see Luhn *et al.* 1984), but this will not affect the model calculations below since we select a temperature range broad enough to generate *all* resonantly heated Fe charge states.

composition is a reflection of the ambient source composition (e.g., Zwickl *et al.* 1978). A specific mechanism suggested by Gloeckler *et al.* (1975) was enrichment of heavy ions in the lower corona in the presence of thermal gradients which result in thermal diffusion dominating over the pressure gradients (e.g., Geiss 1972, and references therein). These suggestions have been neglected since Fisk (1978) pointed out the possibility that a plasma-resonance <sup>3</sup>He heating mechanism might also heat heavy ions. However, in view of the lack of correlation between the degree of <sup>3</sup>He and heavy-nuclei enrichments reported here, it seems appropriate to reexamine these processes.

Nakada (1969, 1970) has presented model calculations of the lower coronal composition due to transport processes from the photosphere including thermal and pressure gradient effects. Such models produce large enhancements of heavy ions (see also Jokipii 1965, 1966; Delache 1967). Figure 11c displays calculated heavy-element enrichments compared with the source (photosphere) material from the detailed calculations of Nakada (1969, his Fig. 5). A temperature gradient of 1 K cm<sup>-1</sup> at  $T = 10^5$  K was assumed, and the line in Figure 11c covers the *range* of enhancements found from temperatures of  $5 \times 10^5$ – $9 \times 10^5$  K (at higher temperatures the functional form assumed for heavy-ion ionization states was inappropriate). The pattern appearing in Nakada's calculation is a surprisingly good fit to our observed heavy-ion enhancements in <sup>3</sup>He-rich events, and is all the more interesting because basically the *same* enrichment pattern is observed over a broad temperature range. An enrichment pattern which occurs over such a wide range of temperatures is consistent with our observations of essentially a single enrichment pattern in almost all of the <sup>3</sup>He-rich events in our survey.

It should be pointed out that the enhancements in Nakada's calculation were with respect to a photospheric composition; however, if the same physical conditions applied in the corona, then the enhancements would be with respect to the coronal composition which closely resembles the large flare particle abundances used here as the reference. In addition, we note that H and <sup>4</sup>He are much more strongly depleted in this model (e.g., they are less abundant than O) than in our observations; clearly, then, if Coulomb friction models are invoked to explain the heavy-ion enrichments, other mechanisms must be responsible for the H and <sup>4</sup>He abundances.

#### V. DISCUSSION

It has been shown in the previous section that the heavy-nuclei enrichment pattern observed in <sup>3</sup>He-rich events can be generally reproduced by simple models based on plasma heating, and also by mechanisms based on thermal diffusion. We now examine to what extent these models are consistent with the *other* observational features summarized in § IIIe, and also observations of the particle ionization states reported in other studies.

The simple plasma resonance model was able to reproduce the enrichment pattern observed, but rather minor modifications of some of the model parameters produced enhancement patterns different from any of those observed in our large sample of events. It is difficult to reconcile this property with the fact that the <sup>3</sup>He-rich events have a *characteristic* enrichment pattern for heavy nuclei: one might expect to see large variations in the heavy-nuclei abundance patterns if this were the case. This is probably a general feature of such resonance models: if they are, on the one hand, capable of producing

enrichments of <sup>3</sup>He with respect to <sup>4</sup>He of  $10^3$ – $10^4$ , they will probably also be capable of producing dramatic heavy-ion abundance enrichments and variations—but this property is *not* observed in the events. Similarly, if it is assumed that the heavy-nuclei enhancements are produced by the same physical mechanism which enhances the <sup>3</sup>He, then it is difficult to understand why the degree of <sup>3</sup>He enrichment is uncorrelated with the degree of heavy-nuclei enrichments. Thus, the plasma resonance models appear unattractive as an explanation for the heavy nucleus enrichments observed in these events.

The thermal diffusion model might provide a plausible explanation for our observations *if* it is assumed that the mechanisms which enrich <sup>3</sup>He occur in coronal locations which are typically enhanced with heavy elements. Such an association might not be unexpected: for the example in the Fisk (1978) model the operative plasma resonance *requires* a rather large helium abundance ( $n_{\text{He}}/n_{\text{H}} \approx 0.3$ ). The same processes which would tend to concentrate helium would also concentrate heavier elements as shown, e.g., in Nakada's model. The fact that Nakada's (1969) calculations produced virtually the same enhancement pattern over a broad range of temperatures is entirely consistent with the observation of an enhancement pattern that is basically the same for all the <sup>3</sup>He-rich events. However, the Nakada model considered temperatures only up to  $\sim 10^6$  K, while the recent observations of Klecker *et al.* (1983) of Fe charge states of  $19.5 \pm 1.5$  and Luhn *et al.* (1985) of fully stripped Si indicate source regions with temperatures  $> 5 \times 10^6$  K for <sup>3</sup>He-rich flares.<sup>3</sup> It is not clear whether or not the enhancements of heavy elements in the Nakada model would persist at these higher temperatures. If the high ionization states of Fe are indeed indicators of the source plasma temperature, then the source location could be rather high in the corona. Such high coronal locations for these events might help the accelerated particles gain access to interplanetary magnetic field lines. We note that Kahler *et al.* (1985a) have also suggested a high coronal location for <sup>3</sup>He-rich events based on their association with kilometric type III radio bursts.

In summary, our new observations, along with previously reported properties of these <sup>3</sup>He-rich events, indicate that while a plasma resonance mechanism may well account for the dramatic <sup>3</sup>He enrichments observed in these events, this mechanism does not appear to be an attractive one for explaining the associated heavy-nuclei enrichments. Rather, the heavy-nuclei enrichments appear to be due to enrichments in the ambient plasma preexisting at the sites where the <sup>3</sup>He-rich events occur. Model calculations of thermal diffusion effects by Nakada (1969) indicate that there may well be such sites routinely occurring in the corona. Although the heavy-nuclei enrichments have been calculated only for the lower corona (where temperature gradients are large), the Fe charge states (Klecker *et al.* 1983) indicate a higher coronal source, which might help explain how the particles from these small particle events escape into interplanetary space.

We are grateful to the many dedicated individuals at the Max-Planck-Institut, the University of Maryland, and the Goddard Space Flight Center, who contributed to the success of the *ISEE 3* instruments and mission. We thank J. Geiss, G.

<sup>3</sup> Such high Fe and Si charge states are also significantly above the optimal ionization states for enrichment in the Fisk (1978) plasma resonance model.

Gloeckler, D. Hamilton, J. Hollweg, P. Nakada, K. Ogilvie, S. Riyopoulos, and L. Vlahos for helpful discussions. One of us (G. M.) wishes to acknowledge the hospitality of the Max-

Planck-Institut, Garching, and the Applied Physics Laboratory/Johns Hopkins University, where a portion of this work was performed.

## REFERENCES

- Anders, E., and Ebihara, M. 1982, *Geochim et Cosmochim.*, **46**, 2363.
- Anglin, J. D. 1975, *Ap. J.*, **198**, 733.
- Anglin, J. D., Dietrich, W. F., and Simpson, J. A. 1977, *Proc. 15th Internat. Cosmic Ray Conf. (Plovdiv)*, **5**, 43.
- Breneman, H., and Stone, E. C. 1985, *Proc. 19th Internat. Cosmic Ray Conf. (La Jolla)*, **4**, 213.
- Cook, W. R., Stone, E. C., Vogt, R. E., Trainor, J. H., and Webber, W. R. 1979, *Proc. 16th Internat. Cosmic Ray Conf. (Kyoto)*, **12**, 265.
- Coplan, M. A., Ogilvie, K. W., Bochsler, P., and Geiss, J. 1984, *Solar Phys.*, **93**, 415.
- Delache, P. 1967, *Ann. Astr.*, **30**, 827.
- Dietrich, W. F. 1973, *Ap. J.*, **180**, 955.
- Ellison, D. C., and Ramaty, R. 1985, *Ap. J.*, **298**, 400.
- Evenson, P., Meyer, P., Yanagita, S., and Forrest, D. J. 1984, *Ap. J.*, **283**, 439.
- Fisk, L. A. 1978, *Ap. J.*, **224**, 1048.
- . 1979, *Proc. 16th Internat. Cosmic Ray Conf. (Kyoto)*, **5**, 134.
- Forman, M. A., Ramaty, R., and Zweibel, E. G. 1985, in *The Physics of the Sun*, ed. P. A. Sturrock (Dordrecht: Reidel), pp. 251–291.
- Foukal, P. V. 1976, *Ap. J.*, **210**, 575.
- Garrard, T. L., Stone, E. C., and Vogt, R. E. 1973, in *Proc. Symposium on High Energy Phenomena on the Sun*, ed. R. Ramaty and R. G. Stone (NASA SP-342), p. 341.
- Geiss, J. 1972, in *Solar Wind*, ed. C. P. Sonnet, P. J. Coleman, Jr., and J. M. Wilcox (NASA SP-308), p. 559.
- Geiss, J., and Reeves, H. 1972, *Astr. Ap.*, **18**, 126.
- Gloeckler, G., Hovestadt, D., Vollmer, O., and Fan, C. Y. 1975, *Ap. J. (Letters)*, **200**, L45.
- Hempe, H., Müller-Mellin, R., Kunow, H., and Wibberenz, G. 1979, *Proc. 16th Internat. Cosmic Ray Conf. (Kyoto)*, **5**, 95.
- Hovestadt, D., et al. 1978, *IEEE Trans. Geosci. Electronics*, **GE-16**, 166.
- Hovestadt, D., Klecker, B., Vollmer, O., Gloeckler, G., and Fan, C. Y. 1975, *Proc. 14th Internat. Cosmic Ray Conf. (Munich)*, **5**, 1613.
- Hsieh, K. C., and Simpson, J. A. 1970, *Ap. J. (Letters)*, **162**, L191.
- Hurford, G. J., Mewaldt, R. A., Stone, E. C., and Vogt, R. E. 1975, *Ap. J. (Letters)*, **201**, L95.
- Ibragimov, I. A., and Kocharov, G. E. 1977, *Proc. 15th Internat. Cosmic Ray Conf. (Plovdiv)*, **11**, 340.
- Jokipii, J. R. 1965, Ph.D. thesis, California Institute of Technology.
- . 1966, in *The Solar Wind*, ed. R. J. Mackin and M. Neugebauer (New York: Pergamon), p. 215.
- Jordan, C. 1969, *M.N.R.A.S.*, **142**, 501.
- Kahler, S. W., Lin, R. P., Reames, D. V., Stone, R. G., and Liggett, M. 1985a, *Proc. 19th Internat. Cosmic Ray Conf. (La Jolla)*, **4**, 269.
- Kahler, S., Reames, D. V., Sheeley, N. R., Jr., Howard, R. A., Koomen, M. J., and Michels, D. J. 1985b, *Ap. J.*, **290**, 742.
- Klecker, B., Hovestadt, D., Gloeckler, G., Möbius, E., Ipavich, F. M., and Scholer, M. 1983, *Proc. 18th Internat. Cosmic Ray Conf. (Bangalore)*, **10**, 330.
- Kocharov, L. G., and Kocharov, G. E. 1981, A. F. Ioffe Physico-Technical Institute, Leningrad, preprint No. 722.
- Kocharov, L. G., and Kocharov, G. E. 1984, *Space Sci. Rev.*, **38**, 89.
- Kocharov, L. G., and Orishchenko, A. V. 1983, *Proc. 18th Internat. Cosmic Ray Conf. (Bangalore)*, **4**, 37.
- . 1985, *Proc. 19th Internat. Cosmic Ray Conf. (La Jolla)*, **4**, 293.
- Lin, R. P., Mewaldt, R. A., and Van Hollebeke, M. A. I. 1982, *Ap. J.*, **253**, 949.
- Luhn, A., Klecker, B., Hovestadt, D., Gloeckler, G., Ipavich, F. M., Scholer, M., Fan, C. Y., and Fisk, L. A. 1984, *Adv. Space Res.*, **4**, 161.
- Luhn, A., Klecker, B., Hovestadt, D., and Möbius, E. 1985, *Proc. 19th Internat. Cosmic Ray Conf. (La Jolla)*, **4**, 285.
- Mason, G. M., Fisk, L. A., Hovestadt, D., and Gloeckler, G. 1980, *Ap. J.*, **239**, 1070.
- Mason, G. M., Gloeckler, G., and Hovestadt, D. 1979a, *Proc. 16th Internat. Cosmic Ray Conf. (Kyoto)*, **5**, 128.
- . 1979b, *Ap. J. (Letters)*, **231**, L87.
- Mason, G. M., Reames, D. V., Hovestadt, D., and von Roseninge, T. T. 1985, *Proc. 19th Internat. Cosmic Ray Conf. (La Jolla)*, **4**, 281.
- Mason, G. M., Reames, D. V., von Roseninge, T. T., Klecker, B., and Hovestadt, D. 1984, *Trans. Am. Geophys. U.*, **65**, 1036.
- Ma Sung, L. S., Gloeckler, G., Fan, C. Y., and Hovestadt, D. 1981, *Ap. J. (Letters)*, **245**, L45.
- McGuire, R. E., von Roseninge, T. T., and McDonald, F. B. 1979a, *Proc. 16th Internat. Cosmic Ray Conf. (Kyoto)*, **5**, 61.
- . 1979b, *Proc. 16th Internat. Cosmic Ray Conf. (Kyoto)*, **5**, 90.
- Mewaldt, R. A. 1980, in *Proc. Conf. Ancient Sun*, ed. R. O. Pepin, J. A. Eddy, and R. B. Merrill (New York: Pergamon), p. 81.
- Meyer, J. P. 1985, *Ap. J. Suppl.*, **57**, 151.
- Möbius, E., Hovestadt, D., Klecker, B., and Gloeckler, G. 1980, *Ap. J.*, **238**, 768.
- Möbius, E., Scholer, M., Hovestadt, D., Klecker, B., and Gloeckler, G. 1982, *Ap. J.*, **259**, 397.
- Nakada, M. P. 1969, *Solar Phys.*, **7**, 302.
- . 1970, *Solar Phys.*, **14**, 457.
- Ogilvie, K. W., Durney, A., and von Roseninge, T. T. 1978, *IEEE Trans. Geosci. Electronics*, **GE-16**, 151.
- Ramaty, R., et al. 1980, in *Solar Flares: A Monograph from the Skylab Workshop II*, ed. P. A. Sturrock (Boulder: Colorado Ass. University Press), p. 117.
- Reames, D. V., and von Roseninge, T. T. 1981, *Proc. 17th Internat. Cosmic Ray Conf. (Paris)*, **3**, 162.
- . 1983, *Proc. 18th Internat. Cosmic Ray Conf. (Bangalore)*, **4**, 48.
- Reames, D. V., von Roseninge, T. T., and Lin, R. P. 1985, *Ap. J.*, **292**, 716.
- Serlemitsos, A. T., and Balasubrahmanyam, V. K. 1975, *Ap. J.*, **198**, 195.
- Shull, J. M., and Van Steenberg, M. 1982, *Ap. J. Suppl.*, **48**, 95.
- Sullivan, J. D. 1971, *Nucl. Instr. Methods*, **95**, 5.
- Varvoglis, H., and Papadopoulos, K. 1983, *Ap. J. (Letters)*, **270**, L95.
- von Roseninge, T. T., McDonald, F. B., Trainor, J. H., Van Hollebeke, M. A. I., and Fisk, L. A. 1978, *IEEE Trans. Geosci. Electronics*, **GE-16**, 208.
- Weatherall, J. 1984, *Ap. J.*, **281**, 468.
- Zwickl, R. D., Roelof, E. C., Gold, R. E., Krimigis, S. M., and Armstrong, T. P. 1978, *Ap. J.*, **225**, 281.

D. HOVESTADT and B. KLECKER: Max-Planck-Institut für Physik und Astrophysik, Institut für Extraterrestrische Physik, D-8046 Garching, München, West Germany

G. M. MASON: Department of Physics and Astronomy, University of Maryland, College Park, MD 20742

D. V. REAMES and T. T. VON ROSENINGE: Code 661, Laboratory for High Energy Astrophysics, NASA, GSFC, Greenbelt, MD 20771